Cytogenet Genome Res 106:61–67 (2004)
DOI: 10.1159/000078563

Cytogenetic and Genome Research

Cloning and characterization of an inversion breakpoint at 6q23.3 suggests a role for Map7 in sacral dysgenesis

R. Sood,[a] P.I. Bader,[b] M.C. Speer,[c] Y.H. Edwards,[d] E.M. Eddings,[a] R.T. Blair,[e] P. Hu,[a] M.U. Faruque,[a] C.M. Robbins,[a] H. Zhang,[a] J. Leuders,[a] K. Morrison,[d] D. Thompson,[f] P.L. Schwartzberg,[e] P.S. Meltzer,[a] and J.M. Trent[a]

[a] Cancer Genetics Branch, National Human Genome Research Institute, National Institutes of Health, Bethesda, MD; [b] Northeast Indiana Genetic Counseling Center, Fort Wayne, IN; [c] Duke University Medical Center, Durham, NC (USA); [d] MRC Human Biochemical Genetics Unit, Biology Department, University College London, London (UK); [e] Genetic Disease Research Branch, National Human Genome Research Institute, National Institutes of Health, Bethesda, MD (USA); [f] Department of Neurosurgery, Great Ormond Street Hospital for Children, London (UK)

Abstract. Here we report on a male patient with sacral dysgenesis (SD) and constitutional pericentric inversion of chromosome 6 (p11.2;q23.3). SD is a heterogeneous group of congenital anomalies with complex genetic etiology. Previously, a patient with sacral abnormalities and an interstitial deletion of 6q23→q25 region has been described. We speculated that a susceptibility gene for SD lies in 6q23.3 region (disrupted in both patients), and therefore, cloning of the breakpoint in our patient would lead to the identification of the disrupted gene. We performed FISH analysis followed by Southern blot analysis and inverse PCR to clone the breakpoint. The 6p11.2 breakpoint mapped very close to the centromere, and the 6q23.3 breakpoint localized in the ninth intron of the MAP7 gene. We then evaluated the involvement of MAP7 in SD by further screening of the gene in several patients with a similar phenotype. Two nucleotide changes causing Ile257Asn and Glu571Ala substitutions in the protein, both affecting amino acid residues conserved in the mouse homolog, were identified in two patients. Both changes are either very rare polymorphisms or true mutations, since they were not detected in 167 normal individuals nor found in the SNP database. Therefore, our study suggests MAP7 as a candidate gene for SD. However, we were unable to detect any sacral defects in the MAP7 knockout mice.

Copyright © 2004 S. Karger AG, Basel

Sacral dysgenesis (SD), also known as sacral agenesis or caudal regression syndrome, is characterized by the congenital absence of all or part of the sacrum with contiguous caudal defects and associated anomalies (Welch and Aterman, 1984; Pang, 1993). It can occur as an isolated anomaly or with other malformations, such as Currarino syndrome (O'Riordain et al., 1991; Lynch et al., 2000). Embryologically caudal regression or dysgenesis has been ascribed to defective blastogenesis, and there has been overlap between caudal dysgenesis and other conditions believed to be due to errors in blastogenesis such as the VACTERL association (Cuschieri, 2002). The degree of neurologic involvement usually depends on the amount of sacrum present, most often presenting as a neurogenic bladder due to the absence of the corresponding sacral motor nerves (Lotan et al., 1981). Skeletal defects often go undetected unless X-rays are performed due to other symptoms, such as bowel and urine incontinency (Kaneoya et al., 1990; Unluer and Bulut, 1991). Most cases of SD are sporadic, although familial cases have also been reported (Sarica et al., 1998). Sporadic cases of SD are often associated with maternal diabetes (White

The authors gratefully acknowledge support from grants HD33400 and NS39818.

Received 17 December 2003; manuscript accepted 11 February 2004.

Request reprints from: Dr. Raman Sood
NHGRI, NIH, Building 49, Room 3A30
9000 Rockville Pike, Bethesda, MD 20892 (USA)
telephone: +1-301-435-5746; fax: +1-301-402-4929
e-mail: rsood@nhgri.nih.gov.

Current address of J.M.T.: Translational Genomics Research Institute (TGen)
400 North Fifth Street, Suite 1600, Phoenix AZ 85004 (USA).

and Klauber, 1976; Dunn et al., 1981; Sonek et al., 1990). Familial cases display autosomal dominant inheritance with incomplete penetrance (Borrelli et al., 1985; O'Riordain et al., 1991). Cytogenetic studies (Morichon-Delvallez et al., 1993; Savage et al., 1997) and linkage analysis (Lynch et al., 1995) followed by positional cloning efforts has led to the identification of a gene, HLXB9 at 7q36 with mutations in several families with sacral agenesis (Ross et al., 1998). HLXB9 is a homeobox gene that codes for the nuclear protein HB9. The exact mechanism by which mutations in HLXB9 cause defects in caudal development is currently unknown, although most mutations have been observed in the homeobox domain (Belloni et al., 2000; Hagan et al., 2000; Kochling et al., 2001). Mice homozygous for a null mutation in HLXB9 gene do not display any detectable sacral defects (Harrison et al., 1999; Li et al., 1999). Mutations in HLXB9 have been detected in most cases of hereditary sacral agenesis but not in sporadic cases with a similar phenotype (Lynch et al., 2000).

A lack of mutations in HLXB9 in sporadic cases and other reports of non-7q cytogenetic abnormalities and linkage analysis suggest genetic heterogeneity. McLeod and colleagues (McLeod et al., 1990) reported a patient with an interstitial deletion of 6q23 to q25 region and sacral agenesis. Involvement of the T-locus (Brachyury) was also suggested based on the similarities in defects caused by T-locus mutations in the mouse to spina bifida and sacral agenesis in human (Fellous et al., 1982). However, any major role of the T-locus in the etiology of SD was excluded by mutation screening in 28 patients (Papapetrou et al., 1999). These studies indicate complex genetic etiology for SD. In an effort to identify additional candidate genes for sacral dysgenesis, we performed molecular delineation of a constitutional chromosomal aberration involving chromosome 6, inv (6) (p11.2;q23.3) in a patient with clinical symptoms of SD. The rearrangement appeared to be a balanced inversion with no detectable loss of chromosomal material based on cytogenetic analysis using FISH. Here we report the molecular cloning and characterization of the 6q23.3 breakpoint in this patient.

Materials and methods

Case report

This study is based on a newborn male twin diagnosed with sacral dysgenesis by X-ray and MRI examination. The patient exhibited typical symptoms of SD, including absent sacrum, closed lipomeningocele, and anal atresia. The patient also exhibited multiple anomalies of the thoracolumbar vertebrae, tracheoesophageal fistula, and esophagal atresia indicating a wide spectrum of midline defects occasionally seen in SD. Mildly low set ears, arthrogryposis and hypoplasia of the lower extremities and clubfoot were also present. There was no family history of diabetes or teratogen exposure. Cytogenetic studies revealed a pericentric inversion: inv(6)(p11.2;q23.3), also present in the father, an apparently normal male fraternal twin, and the paternal grandfather who suffered from hairy cell leukemia. The father had a congenital neurogenic bladder, indicating a mild form of sacral dysgenesis. A lymphoblastoid cell line established from patient's blood was used in this study after institutional review board approval.

YAC, BAC and PAC clones

YAC clones mapping to 6q23.3 band region were identified from the Whitehead Institute's human physical mapping database (http://www-genome.wi.mit.edu/). Human BAC and PAC libraries (Genome Systems) were screened with STS primers from available genetic markers within the interval. DNA from YAC clones was isolated by spheroplasting as described by Carpten et al. (1994). DNA from BAC and PAC clones was purified using the Autogen 850 automated DNA isolation system using the manufacturer's recommended protocol (Autogen).

Polymerase chain reaction (PCR) and mutation analysis

PCR reactions were performed using 10 ng of template DNA with 2.25 mM Mg^{++}, 250 nM dNTPs, 333 nM each forward and reverse primer, PCR buffer II (Perkin-Elmer), and 0.6 units of AmpliTaq Gold Polymerase (Perkin-Elmer) in a 15-µl total PCR reaction volume. All of the PCR reactions were carried out in a model 9700 Thermocycler (Perkin-Elmer) using the following cycling conditions: initial denaturation of 94 °C for 12 min; 94 °C for 15 s, 55 °C for 15 s, 72 °C for 15 s for 35 cycles; followed by a final extension at 72 °C for 10 min. Mutations in HLXB9 were analyzed by single-strand conformation polymorphism (SSCP) using nine overlapping primer pairs that covered the entire coding sequence. The PCR template was cDNA synthesized from patient RNA using reverse transcriptase AMV and oligo-(dT)15 primer in the presence of RNase-inhibitor (Boehringer Mannheim). Radiolabeled PCR products were electrophoresed in 0.5× MDE™ (FMC Bio Products) gels with and without glycerol at room temperature with 0.6× TBE at 5 W for 16 h. Mutation analysis of MAP7 was performed on genomic DNA from patients using SSCP, denaturing high performance liquid chromatography (dHPLC, Varian), and bidirectional sequencing technologies. Primers were designed to cover all 16 coding exons of the gene and primer sequences are available upon request. Most of the samples were analyzed by dHPLC for 12 exons and sequencing for four exons numbered 10, 13, 15, and 16. A small subset of patients was screened by SSCP for all exons. PCR products representing heteroduplex samples from dHPLC analysis, conformers from SSCP gels, and direct sequencing exons were sequenced using an Applied Biosystems 377 XL automated DNA sequencer (Perkin-Elmer). Sequences were analyzed using Sequencher v4.1 (Gene Codes) to identify nucleotide substitutions.

Fluorescence in situ hybridization (FISH)

Slides with metaphase chromosome spreads were prepared from the patient's lymphoblastoid cell line. All probes were labeled with Spectrum-Orange conjugated dUTP by degenerate oligonucleotide primed-PCR. The slides were treated with RNase for 2 h at 37 °C and were denatured in 70 % formamide/2× SSC at 72 °C for 2 min. Hybridization was performed in a humidity chamber at 37 °C overnight followed by washing and counterstaining with DAPI in antifade.

Southern blot analysis

Southern blots were prepared in the laboratory using standard methods. Briefly, 5 µg of DNA from patient and controls was digested with selected restriction enzymes, electrophoresed on 0.8 % agarose gels, and transferred to GeneScreen plus nylon membranes (Dupont). Probes were labeled using ^{32}P-dCTP using a Prime-it II kit (Stratagene). Hybridization was performed overnight at 65 °C in RapidHyb buffer (Amersham). Blots were washed in 2× SSC, 0.1 % SDS twice at room temperature for 10 min each, followed by a 20-min wash in 0.1× SSC, 0.1 % SDS at 65 °C.

Inverse PCR, cloning and sequencing

Following the localization of breakpoints by Southern blots, the inverse PCR approach was used to amplify junction fragments. Briefly, DNA from patient and a normal control was digested with *Eco*RI, purified using a Qiaquick PCR purification kit (Qiagen), and self-ligated using T4 DNA ligase (Stratagene). Three sets of primers were designed from the 1,430 bp *Eco*RI fragment containing the breakpoint. Each set consisted of a pair of primers facing in opposite directions, 12–18 bp apart. Self-ligated *Eco*RI DNA was purified using the Qiaquick PCR purification kit and was used as template for PCR using each of the three sets of primers. The products were subcloned using a TOPO TA cloning kit (Invitrogen), and sequenced with vector primers followed by walking primers to identify the junction sequences. Sequence analysis was performed using Sequencher.

Mice genotyping and phenotyping

DNA was extracted from mice tails using a standard protocol and was analyzed by PCR for the presence of gene-trap vector. Wild type animals were identified by lack of amplification with vector primers. Further analysis using Southern blots as described by Komada et al. (2000) was used to identi-

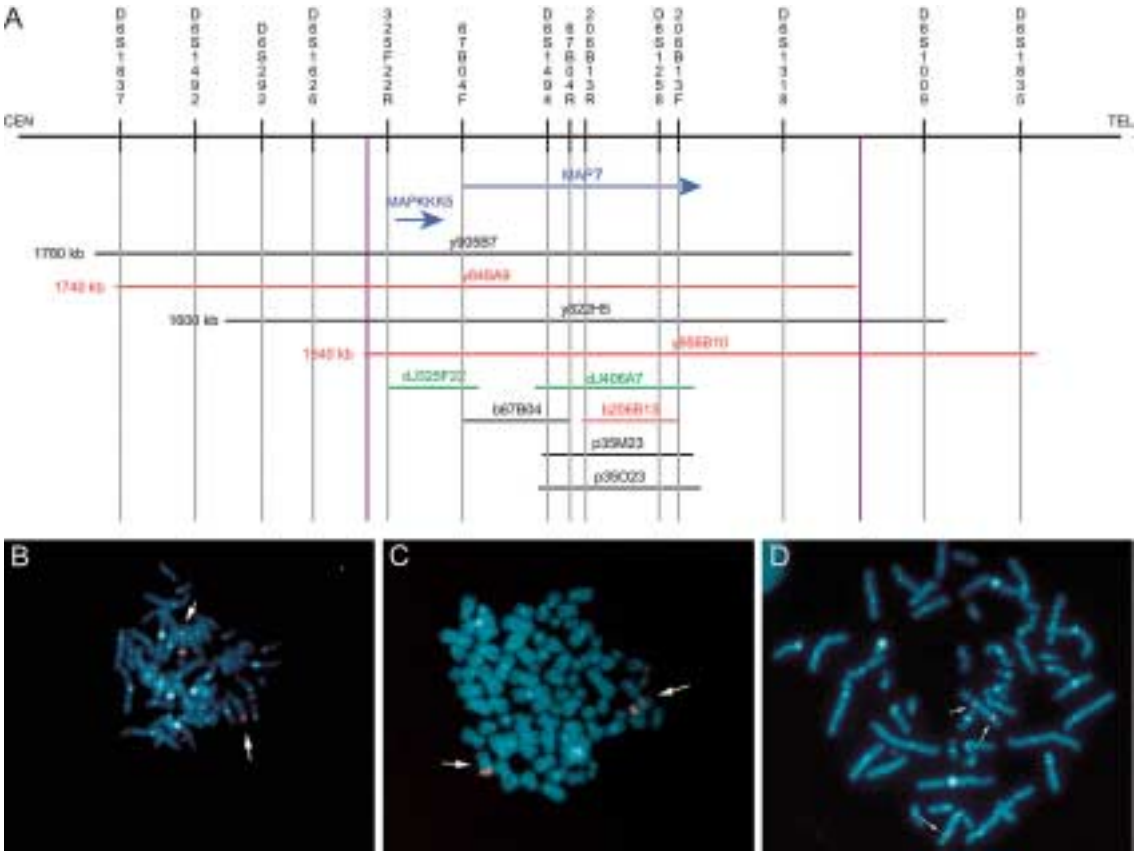

Fig. 1. Breakpoint localization by physical mapping and FISH analysis in the patient's lymphoblastoid cell line. (**A**) Physical map of the 6q23.3 region. YAC and BAC clones used in FISH analysis are shown in red, BAC clones sequenced by the Sanger Center are shown in green and transcripts are shown in blue color. Vertical lines show known STSs representing genetic markers and new STSs derived from BAC end sequences. (**B**) FISH analysis using YAC 848A9. (**C**) FISH analysis using YAC 956B10. (**D**) FISH analysis using BAC 206B13. In **B**, **C**, and **D** arrows point to normal and inversion 6 chromosomes. In all cases, two signals are seen on inv(6) chromosome, indicating that these clones span the breakpoint.

fy homozygous null mice from heterozygote animals. Newborn mice were phenotyped for sacral dysgenesis using radiographs and skeletal staining (Wallin et al., 1994). Radiographs were performed on anesthetized animals using a Faxitron X-ray machine and Kodak X-OMAT TL diagnostic film. Different exposure times and magnifications were used to maximize our chances of detecting abnormalities.

Results

First, we ruled out that the patient's phenotype was due to a mutation in HLXB9 by SSCP analysis of patient's cDNA using nine overlapping primer pairs designed from the coding sequence of HLXB9. Based on the previous report of possible involvement of 6q in SD, and the close proximity of the p arm breakpoint to the centromere (a region often devoid of genes), we hypothesized that the breakpoint at 6q23.3 in this patient's inv(6)(p11.2;q23.3) might have disrupted a gene involved in SD. A physical map of the region was assembled using the Whitehead YAC contig WC-574 and BAC/PAC clones identified by screening genomic libraries with STS markers from the region (Fig. 1A). Two overlapping CEPH-megaYAC clones, y848A9 and y956B10, were found to span the inversion breakpoint by FISH (Fig. 1B, C). BAC and PAC clones from the overlapping region of YACs allowed further refinement of the breakpoint to a single BAC clone, b206B13 (Fig. 1D).

A database search of the end sequences of BAC clone b206B13 identified a 165 kb sequenced BAC clone dJ406A7 (Genbank accession #AL023284). Since this sequence was not annotated, we performed further analysis using GeneMachine (Makalowska et al., 2001) and localized the MAP7 gene (locus-ID: 9053), previously called E-MAP115 or Ensconsin to this region (Masson and Kreis, 1993). By aligning end sequences of our FISH clone b206B13 with the dJ406A7 sequence, we localized the breakpoint to a genomic interval of 89,955 bp most of which was occupied by the MAP7 gene (exon 1 begins at 8,083 bp and exon 17 ends at 85,644 bp). To delineate how the MAP7 gene was disrupted by the breakpoint, we performed a series of genomic Southern blot hybridizations to identify novel junction fragments. We generated nine PCR-derived probes (P1-P9) from repeat-free regions and roughly spaced at 10-kb intervals (Fig. 2A). Using probe 6 (a 938 bp fragment containing exon 7) we identified two additional fragments in the patient's

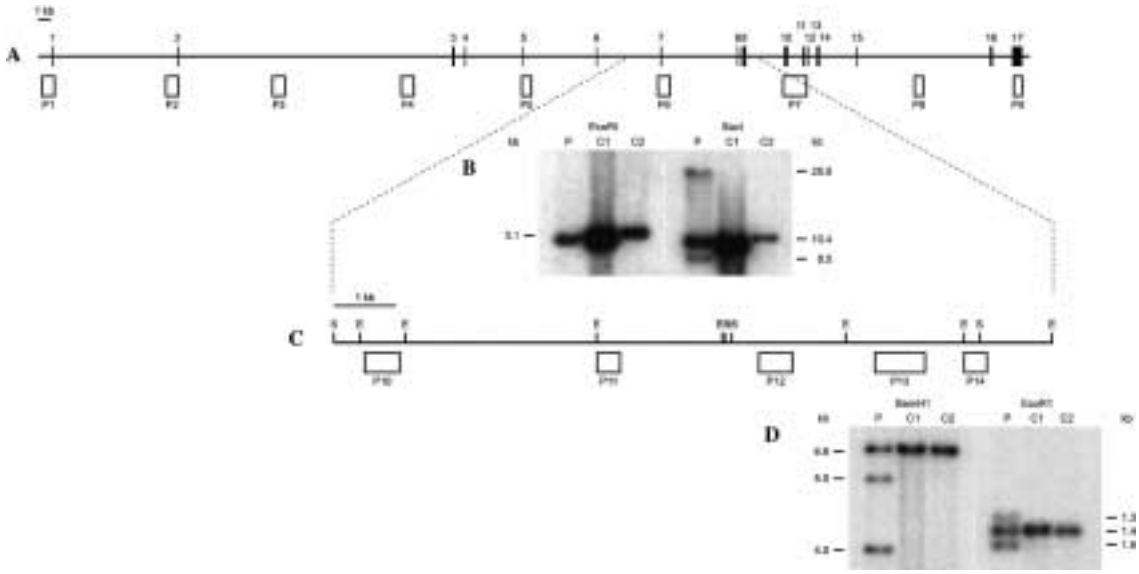

Fig. 2. Breakpoint localization using Southern blot analysis. (**A**) Genomic organization of MAP7. The horizontal line represents the sequence of b206B13. Vertical lines depict exons 1 through 17. Boxes underneath the horizontal line show probes one through nine. (**B**) *Eco*RI and *Sac*I Southern blots using probe 6. Lane P: patient DNA, lanes C1 and C2: DNA from control individuals. The patient DNA shows two additional bands following *Sac*I digest. (**C**) Restriction map of the 10-kb *Sac*I fragment showing probes 10–14 and restriction sites marked as B for *Bam*HI, E for *Eco*RI and S for *SacI* sites. (**D**) *Bam*HI and *Eco*RI Southern blots using probe 14. In both *Bam*HI and *Eco*RI digested DNA, the patient DNA shows two extra bands representing the junction fragments.

DNA digested with the restriction enzyme *Sac*I (as compared to normal controls) (Fig. 2B). These results allowed us to narrow the breakpoint region to a 10,419 bp *Sac*I fragment containing our probe. Five new probes (P10-P14) were then designed from this region allowing us to narrow the breakpoint further to a small *Eco*RI fragment (Fig. 2C). Probe 14 identified rearrangements in both *Bam*HI and *Eco*RI digested proband's DNA (Fig. 2D). This unequivocally localized the breakpoint to a 1,430 bp *Eco*RI fragment. We then used an inverse PCR strategy to clone the junction fragments (Fig. 3A). Analysis of the cloned products identified two junction fragments of 1,331 bp and 1,535 bp corresponding to the two extra bands seen on the Southern blot. Their alignment with the original 1,430 bp sequence localized the breakpoint at position 246 of this *Eco*R1 fragment (Fig. 3B).

As expected, the sequences on either side of the breakpoint mapped to 6p11.1 by using the BLAT search feature of UCSC against the April 2003 assembly of the human genomic sequence. This data maps the 6p11.1 breakpoint very close to the centromere (approximately 58 Mb position on the chromosome). There are no genes, ESTs or predicted transcripts mapping in the vicinity of the p-arm breakpoint, suggesting disruption of MAP7 as the most likely cause of our patient's SD phenotype. The breakpoint in MAP7 lies in the intron between exons 9 and 10, thereby placing the first nine exons of the gene at the centromeric side of the rearrangement.

To further evaluate the role of MAP7 in the etiology of SD, we screened 117 patients with caudal developmental defects for mutations using primers derived from 16 coding exons. In addition to a few common polymorphisms, we detected two rare variants: a T770A change causing Ile257Asn (detected in a patient with lipomyelomeningocele) and an A1712C change leading to Glu571Ala (detected in a patient with lumbar lipomeningocoele). Both nucleotide changes were not detected in any other patient or 167 normal individuals. Unfortunately, no family history or other clinical information was available to track the changes in these cases. However, both changes occur at residues conserved in the mouse. Furthermore, both changes were not found in the SNP database.

During the course of our study, Komada et al. (2000) created a MAP7 knockout mouse using gene-trapping technology and demonstrated the role of this gene in spermatogenesis. Male mice homozygous for the mutation were sterile due to deformation of spermatid nuclei. They also detected a strong expression of MAP7 in the floor plate of the neural tube. The floor plate is important for the development of the spinal cord. Therefore, to analyze these mice for sacral defects, we obtained heterozygous mice from the Fred Hutchison Cancer Research Center and bred them to homozygosity after re-derivation into the NHGRI animal facility. We analyzed newborn mice for sacral dysgenesis using X-rays and skeletal staining. We were not able to identify any phenotypic differences in the sacral region of homozygous mice when compared to wild type and heterozygous animals.

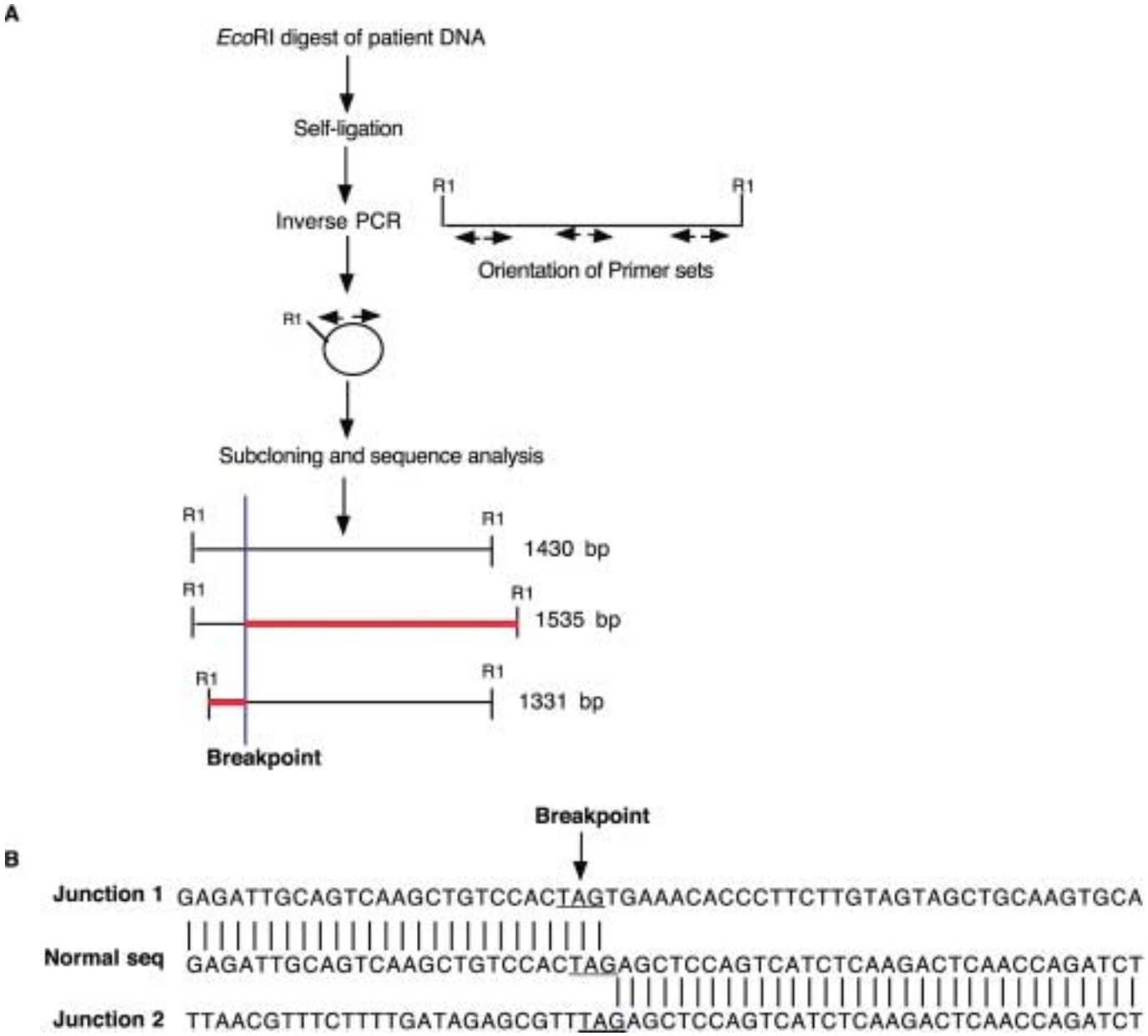

Fig. 3. Breakpoint cloning. (**A**) Flowchart of inverse PCR strategy used in cloning. Junction fragments depicted as horizontal lines are shown in comparison with the expected EcoRI fragment. The red portion of the junction fragments shows the part derived from the centromeric side of the breakpoint. (**B**) Sequence of junction fragments around the breakpoint in comparison with the 6q23.3 sequence showing the exact location of the breakpoint.

Discussion

We report here the disruption of MAP7 as a result of a pericentric inversion in a patient with clinical symptoms of SD and associated anomalies. The patient's father has the same chromosomal rearrangement and a mild form of SD, whereas the patient's fraternal twin brother with the same rearrangement appeared normal at the time of initial examination. A paternal grandfather with the same chromosome rearrangement was not available for evaluation, but was known to have hairy cell leukemia. The immediate question that comes to mind is whether disruption of MAP7 plays a causal role in this patient's phenotype or is a mere coincidence. In order to answer this question we performed mutation screening of MAP7 in additional patients as well as a phenotypic analysis of the knockout mice.

Chromosomal rearrangements have been successfully used in defining molecular defects for several diseases. However, in most cases the rearrangements are recurrent or are verified by the molecular defects at the same locus in other patients. The coexistence of a cytogenetic abnormality in this region and

sacral defects has been demonstrated in at least one additional patient (McLeod et al., 1990). In addition, we have identified missense mutations affecting conserved amino acids in two patients. Taken together, these findings suggest MAP7 as a strong candidate for SD. The patient's twin might not have manifested the phenotype yet due to incomplete penetrance, epigenetic factors, or late manifestations of the milder disease. Since he appeared asymptomatic at the time of examination, X-rays were not taken and he was not followed-up further.

MAP7 belongs to the family of microtubule-associated proteins, a heterogeneous group of proteins involved in cytoskeletal organization that help maintain cellular shape and polarity (Maccioni and Cambiazo, 1995; Vanier et al., 2003). Expression studies at the mRNA and protein levels have shown a high level of MAP7 expression in epithelial cells and moderate expression in neuronal cells (Fabre-Jonca et al., 1998). Burgess and Schroeder (1979) have speculated that several developmental defects, such as spina bifida, might be related to malfunctioning of the cytoskeleton. Not much is known about MAP7 protein structure or the motifs it contains. Therefore, it is difficult to infer the mechanism of action of the mutations we observed. We did not detect any obvious sacral defect in the MAP7 knockout mice. It is worth noting that the knockout mice for HLXB9, the other gene involved in SD, also show normal caudal development (Harrison et al., 1999; Li et al., 1999). Instead these mice show defective pancreas and aberrant specification of motor neurons (Arber et al., 1999; Thaler et al., 1999).

Our breakpoint cloning approach utilized the available human genomic sequence resources to design probes for Southern blotting and primers for inverse PCR thereby eliminating the need to generate genomic libraries or hybrid cell lines segregating the abnormal chromosome as a prerequisite for cloning. Most recurrent chromosomal breakpoints occur in repetitive sequences that function as recombination hotspots (Edelmann et al., 2001; Kurahashi et al., 2003). The centromeric breakpoint in our patient also lies in repeat sequences. However, no repetitive or palindromic sequences were detected around the breakpoint at 6q23.3 suggesting a mechanism other than recombination between two repetitive sequences for the inversion in this patient.

In summary, we have cloned an inversion breakpoint in a patient with symptoms of SD, and we have identified the exact molecular defect involved in this chromosomal rearrangement. Our study suggests MAP7 as a strong candidate for SD. Further studies in other patients with a similar phenotype are required to determine the extent of the role of MAP7 in the etiology of sacral dysgenesis.

Acknowledgements

We thank Dr. Philippe Soriano and Dr. Masayuki Komada for providing MAP7 null mice and probes for genotyping the mice, Dr. Shelley Hoogstraten-Miller and Gene Elliot for help with the mouse work, Ursula Harper for help with sequencing, Dr. Tom I. Bonner for help with dHPLC, Dr. Mondira Kundu for technical advice about skeletal staining, Dr. Catharine Linder for work during early phase of the project, Dr. Izabela Makalowska for sequence analysis using GeneMachine, and Drs. Maximilian Muenke, David Weaver and Jeffrey Nye for providing DNA from patients for MAP7 mutation analysis.

References

Arber S, Han B, Mendelsohn M, Smith M, Jessell TM, Sockanathan S: Requirement for the homeobox gene Hb9 in the consolidation of motor neuron identity. Neuron 23:659–674 (1999).

Belloni E, Martucciello G, Verderio D, Ponti E, Seri M, Jasonni V, Torre M, Ferrari M, Tsui LC, Scherer SW: Involvement of the HLXB9 homeobox gene in Currarino syndrome. Am J Hum Genet 66:312–319 (2000).

Borrelli M, Bruschini H, Nahas WC, Figueiredo JA, Prado MJ, Spinola R, Walligora M, Freire GC, de Goes GM: Sacral agenesis: why is it so frequently misdiagnosed? Urology 26:351–355 (1985).

Burgess DR, Schroeder TE: The cytoskeleton and cytomusculature in embryogenesis – an overview. Methods Achiev Exp Pathol 8:171–189 (1979).

Carpten JD, DiDonato CJ, Ingraham SE, Wagner-McPherson C, Nieuwenhuijsen BW, Wasmuth JJ, Burghes AH: A YAC contig of the region containing the spinal muscular atrophy gene (SMA): identification of an unstable region. Genomics 24:351–356 (1994).

Cuschieri A and EUROCAT Working Group: Anorectal anomalies associated with or as part of other anomalies. Am J Med Genet 110:122–130 (2002).

Dunn V, Nixon GW, Jaffe RB, Condon VR: Infants of diabetic mothers: radiographic manifestations: Am J Roentgenol 137:123–128 (1981).

Edelmann L, Spiteri E, Koren K, Pulijaal V, Bialer MG, Shanske A, Goldberg R, Morrow BE: AT-rich palindromes mediate the constitutional t(11;22) translocation. Am J Hum Genet 68:1–13 (2001).

Fabre-Jonca N, Allaman JM, Radlgruber G, Meda P, Kiss JZ, French LE, Masson D: The distribution of murine 115-kDa epithelial microtubule-associated protein (E-MAP-115) during embryogenesis and in adult organs suggests a role in epithelial polarization and differentiation. Differentiation 63:169–180 (1998).

Fellous M, Boue J, Malbrunot C, Wollman E, Sasportes M, Van Cong N, Marcelli A, Rebourcet R, Hubert C, Demenais F, Elston RC, Namboodiri KK, Kaplan EB, Fellous M: A five-generation family with sacral agenesis and spina bifida: possible similarities with the mouse T-locus. Am J Med Genet 12:465–487 (1982).

Hagan DM, Ross AJ, Strachan T, Lynch SA, Ruiz-Perez V, Wang YM, Scambler P, Custard E, Reardon W, Hassan S, Nixon P, Papapetrou C, Winter RM, Edwards Y, Morrison K, Barrow M, Cordier-Alex MP, Correia P, Galvin-Parton PA, Gaskill S, Gaskin KJ, Garcia-Minaur S, Gereige R, Hayward R, Homfray T: Mutation analysis and embryonic expression of the HLXB9 Currarino syndrome gene. Am J Hum Genet 66:1504–1515 (2000).

Harrison KA, Thaler J, Pfaff SL, Gu H, Kehrl JH: Pancreas dorsal lobe agenesis and abnormal islets of Langerhans in Hlxb9-deficient mice. Nat Genet 23:71–75 (1999).

Kaneoya F, Mine M, Ishizaka K, Gotoh S, Yokokawa M, Hiraga S: Neurogenic bladder dysfunction due to spina bifida and sacral dysgenesis manifested itself in middle age. Report of a case. Nippon Hinyokika Gakkai Zasshi 81:1091–1094 (1990).

Kochling J, Karbasiyan M, Reis A: Spectrum of mutations and genotype-phenotype analysis in Currarino syndrome. Eur J Hum Genet 9:599–605 (2001).

Komada M, McLean DJ, Griswold MD, Russell LD, Soriano P: E-MAP-115, encoding a microtubule-associated protein, is a retinoic acid-inducible gene required for spermatogenesis. Genes Dev 14:1332–1342 (2000).

Kurahashi H, Shaikh T, Takata M, Toda T, Emanuel BS: The constitutional t(17;22): another translocation mediated by palindromic AT-rich repeats. Am J Hum Genet 72:733–738 (2003).

Li H, Arber S, Jessell TM, Edlund H: Selective agenesis of the dorsal pancreas in mice lacking homeobox gene *Hlxb9*. Nat Genet 23:67–70 (1999).

Lotan D, Hertz M, Aladjem M, Braf Z, Boichis H: Sacral agenesis. Isr J Med Sci 17:437–440 (1981).

Lynch SA, Bond PM, Copp AJ, Kirwan WO, Nour S, Balling R, Mariman E, Burn J, Strachan T: A gene for autosomal dominant sacral agenesis maps to the holoprosencephaly region at 7q36. Nat Genet 11:93–95 (1995).

Lynch SA, Wang Y, Strachan T, Burn J, Lindsay S: Autosomal dominant sacral agenesis: Currarino syndrome. J Med Genet 37:561–566 (2000).

Maccioni RB, Cambiazo V: Role of microtubule-associated proteins in the control of microtubule assembly. Physiol Rev 75:835–864 (1995).

Makalowska I, Ryan JF, Baxevanis AD: GeneMachine: gene prediction and sequence annotation. Bioinformatics 17:843–844 (2001).

Masson D, Kreis TE: Identification and molecular characterization of E-MAP-115, a novel microtubule-associated protein predominantly expressed in epithelial cells. J Cell Biol 123:357–371 (1993).
McLeod DR, Fowlow SB, Robertson A, Samcoe D, Burgess I, Hoo JJ: Chromosome 6q deletions: a report of two additional cases and a review of the literature. Am J Med Genet 35:79–84 (1990).
Morichon-Delvallez N, Delezoide AL, Vekemans M: Holoprosencephaly and sacral agenesis in a fetus with a terminal deletion 7q36 → 7qter. J Med Genet 30:521–524 (1993).
O'Riordain DS, O'Connell PR, Kirwan WO: Hereditary sacral agenesis with presacral mass and anorectal stenosis: the Currarino triad. Br J Surg 78: 536–538 (1991).
Pang D: Sacral agenesis and caudal spinal cord malformations. Neurosurgery 32:755–779 (1993).
Papapetrou C, Drummond F, Reardon W, Winter R, Spitz L, Edwards YH: A genetic study of the human T gene and its exclusion as a major candidate gene for sacral agenesis with anorectal atresia. J Med Genet 36:208–213 (1999).
Ross AJ, Ruiz-Perez V, Wang Y, Hagan DM, Scherer S, Lynch SA, Lindsay S, Custard E, Belloni E, Wilson DI, et al: A homeobox gene, HLXB9, is the major locus for dominantly inherited sacral agenesis: Nat Genet 20:358–361 (1998).
Sarica K, Pinar T, Sarica N, Yagci F, Eryigit M: Sacral agenesis in siblings. Urol Int 60:254–257 (1998).
Savage NM, Maclachlan NA, Joyce CA, Moore IE, Crolla JA: Isolated sacral agenesis in a fetus monosomic for 7q36.1 → qter. J Med Genet 34:866–868 (1997).
Sonek JD, Gabbe SG, Landon MB, Stempel LE, Foley MR, Shubert-Moell K: Antenatal diagnosis of sacral agenesis syndrome in a pregnancy complicated by diabetes mellitus. Am J Obstet Gynecol 162: 806–808 (1990).
Thaler J, Harrison K, Sharma K, Lettieri K, Kehrl J, Pfaff SL: Active suppression of interneuron programs within developing motor neurons revealed by analysis of homeodomain factor HB9. Neuron 23:675–687 (1999).
Unluer E, Bulut F: Sacral agenesis with imperforate anus and its late complication: neuropathic bladder. Int Urol Nephrol 23:341–343 (1991).
Vanier M-T, Deck P, Stutzman J, Gendry P, Arnold C, Dirrig-Grosch S, Kedinger M, Launay J-F: Expression and distribution of distinct variants of E-MAP-115 during proliferation and differentiation of human intestinal epithelial cells. Cell Motil Cytoskeleton 55:221–231 (2003).
Wallin J, Wilting J, Koseki H, Fritsch R, Christ B, Balling R: The role of Pax-1 in axial skeleton development. Development 120:1109–1121 (1994).
Welch JP, Aterman K: The syndrome of caudal dysplasia: a review, including etiologic considerations and evidence of heterogeneity. Pediatr Pathol 2:313–327 (1984).
White RI, Klauber GT: Sacral agenesis: Analysis of 22 cases. Urology 8:521–525 (1976).

Copyright: S. Karger AG, Basel 2004. Reproduced with the permission of S. Karger AG, Basel. Further reproduction or distribution (electronic or otherwise) is prohibited without permission from the copyright holder.